Search for anisotropies in the arrival directions of Ultrahigh Energy Cosmic Rays

Rogerio M. de Almeida, for the Pierre Auger Collaboration
Universidade Federal Fluminense

XI International Conference on New Frontiers in Physics – Crete, Greece, 2022

Pierre Auger Observatory

- ❑ Particles with E > 10^{18} eV
- ❑ **Pierre Auger Observatory**
  - ★ Malargue - Mendoza, Argentir
  - ★ Largest UHECR experiment bu ~ 3000 km^2
- ❑ **Main techniques:**
  - ➔ **Fluorescence detector (FD)**
  - ➔ **Surface detector (SD)**

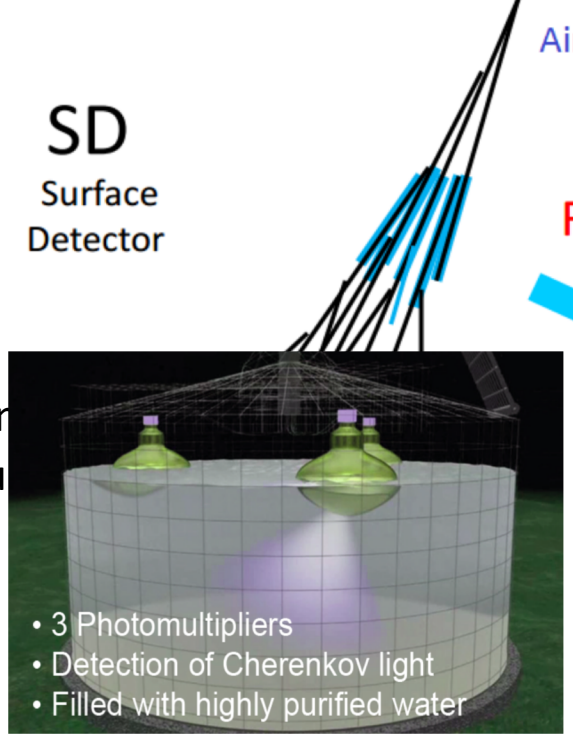

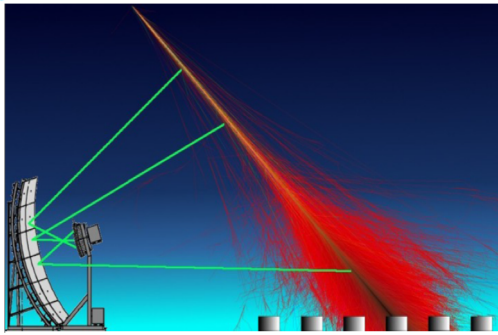

- 1660 water Cherenkov
- 100% duty cycle
- Lateral profile

- 27 telescopes
- 15% duty cycle
- Longitudinal profile

The study of anisotropies is important to understand the origin of UHECR

- **Large Scale Anisotropies**
  - Science 357 (2017) 1266
  - Astrophys. J. 868 (2018) 4
  - Last update: R. M. de Almeida [Auger Collab.] ICRC 2021

- **Intermediate-scale anisotropies**
  - ApJ.Lett. 853:L29 (2018)
  - Accepted for publication in ApJS

Large scale: weighted harmonic analysis

- Search for harmonic modulation in right ascension and azimuth: $x = \alpha$ or ϕ
- Fourier coefficients of order k (1 or 2): $a_x^k = \frac{2}{\mathcal{N}} \sum_{i=1}^{N} w_i \cos(k x_i),\ b_x^k = \frac{2}{\mathcal{N}} \sum_{i=1}^{N} w_i \sin(k x_i)$
- amplitude $r_k^x = \sqrt{(a_k^x)^2 + (b_k^x)^2}$, phase $\varphi_k^x = \frac{1}{k} \tan^{-1} \frac{b_k^x}{a_k^x}$
- weights: small variations in coverage and tilt of the array

$$w_i = \left[\Delta N_{cell}(\alpha_i^0)(1 + 0.003 \tan\theta_i \cos(\phi_i - \phi_0))\right]^{-1}$$

number of active detector cells

right ascension of the zenith of the observatory

average tilt of the array $\phi_0 = -30^\circ$

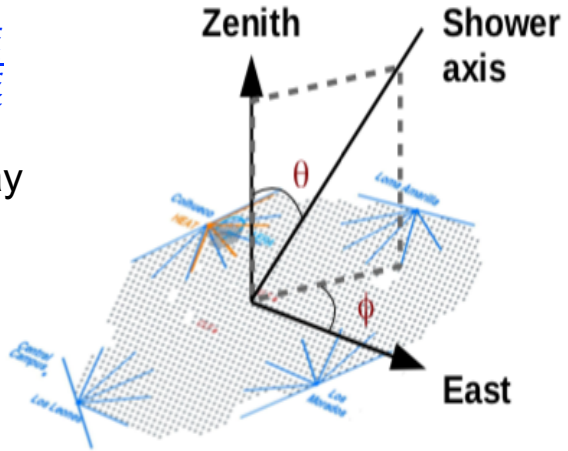

For dipolar modulation, $d_\perp \simeq \frac{r_1^\alpha}{\langle \cos\delta \rangle}$ and $d_z \simeq \frac{b_1^\phi}{\langle \sin\theta \rangle \cos l_{obs}}$

Dipole reconstruction

E (EeV)	N	$d_\perp$	d_z	d	$\alpha_d[^\circ]$	$\delta_d[^\circ]$	$P(\geq r_1^\alpha)$
4-8	106, 290	$0.01^{+0.006}_{-0.004}$	-0.012 ± 0.008	$0.016^{+0.008}_{-0.005}$	97 ± 29	-48^{+23}_{-22}	1.4×10^{-1}
8-16	32, 794	$0.055^{+0.011}_{-0.009}$	-0.03 ± 0.01	$0.063^{+0.013}_{-0.009}$	95 ± 10	-28^{+12}_{-13}	3.1×10^{-7}
16-32	9, 156	$0.072^{+0.021}_{-0.016}$	-0.07 ± 0.03	$0.10^{+0.03}_{-0.02}$	81 ± 15	-43^{+14}_{-14}	7.5×10^{-4}
≥8	44, 398	$0.059^{+0.009}_{-0.008}$	-0.042 ± 0.013	$0.073^{+0.011}_{-0.009}$	95 ± 8	-36^{+9}_{-9}	5.1×10^{-11}
≥32	2, 448	$0.11^{+0.04}_{-0.03}$	-0.12 ± 0.05	$0.16^{+0.05}_{-0.04}$	139 ± 19	-47^{+16}_{-15}	1.0×10^{-2}

was 1.4×10^{-9} (ApJ 2020) and 2.6×10^{-8} (Science 2017)

Corresponds to 6.6σ

$E \geq 8$ EeV

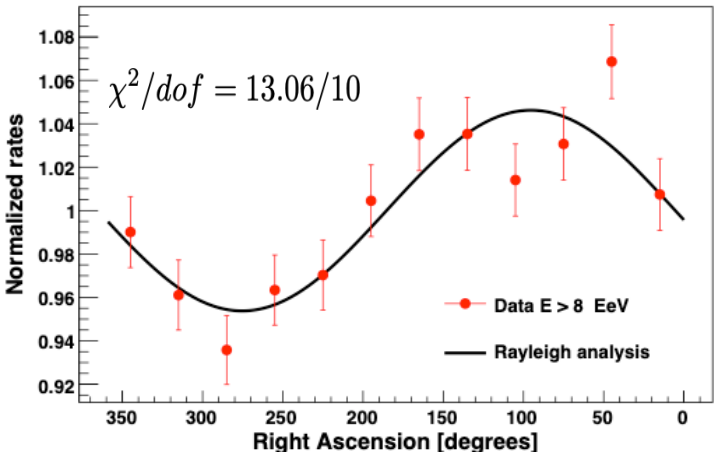

Smoothed by a top-hat window with 45° of radius

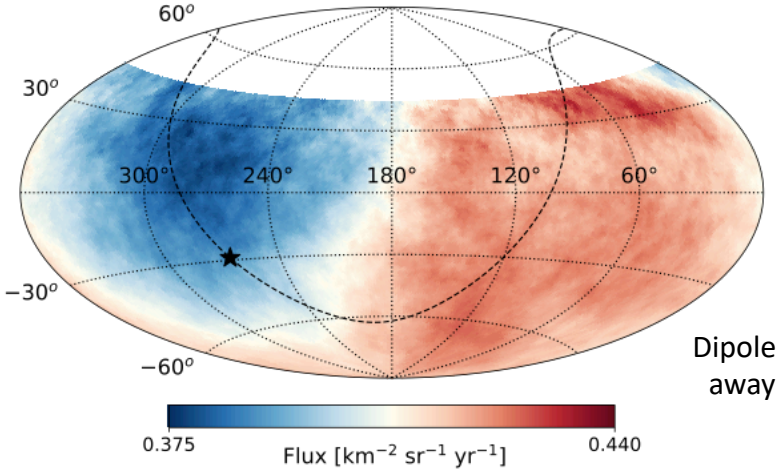

Dipole points ~115° away from the GC

Dipole reconstruction

E (EeV)	N	$d_\perp$	d_z	d	$\alpha_d[^\circ]$	$\delta_d[^\circ]$	$\mathrm{P}(\geq r_1^\alpha)$
4-8	106, 290	$0.01^{+0.006}_{-0.004}$	-0.012 ± 0.008	$0.016^{+0.008}_{-0.005}$	97 ± 29	-48^{+23}_{-22}	1.4×10^{-1}
8-16	32, 794	$0.055^{+0.011}_{-0.009}$	-0.03 ± 0.01	$0.063^{+0.013}_{-0.009}$	95 ± 10	-28^{+12}_{-13}	3.1×10^{-7}
16-32	9, 156	$0.072^{+0.021}_{-0.016}$	-0.07 ± 0.03	$0.10^{+0.03}_{-0.02}$	81 ± 15	-43^{+14}_{-14}	7.5×10^{-4}
≥8	44, 398	$0.059^{+0.009}_{-0.008}$	-0.042 ± 0.013	$0.073^{+0.011}_{-0.009}$	95 ± 8	-36^{+9}_{-9}	5.1×10^{-11}
≥32	2, 448	$0.11^{+0.04}_{-0.03}$	-0.12 ± 0.05	$0.16^{+0.05}_{-0.04}$	139 ± 19	-47^{+16}_{-15}	1.0×10^{-2}

was 1.4×10^{-9} (ApJ 2020) and 2.6×10^{-8} (Science 2017)

Corresponds to 6.6σ

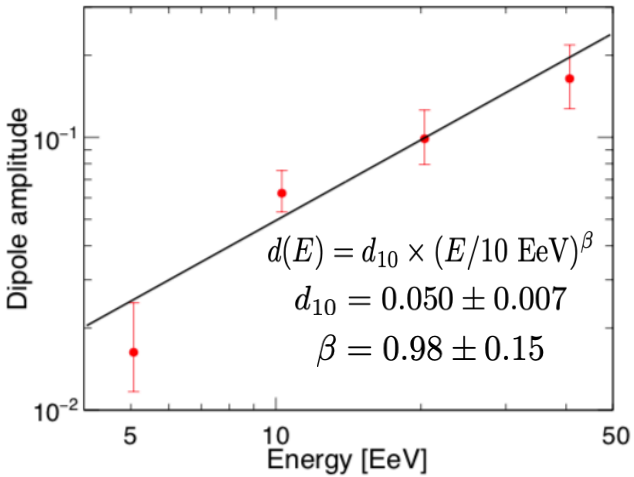

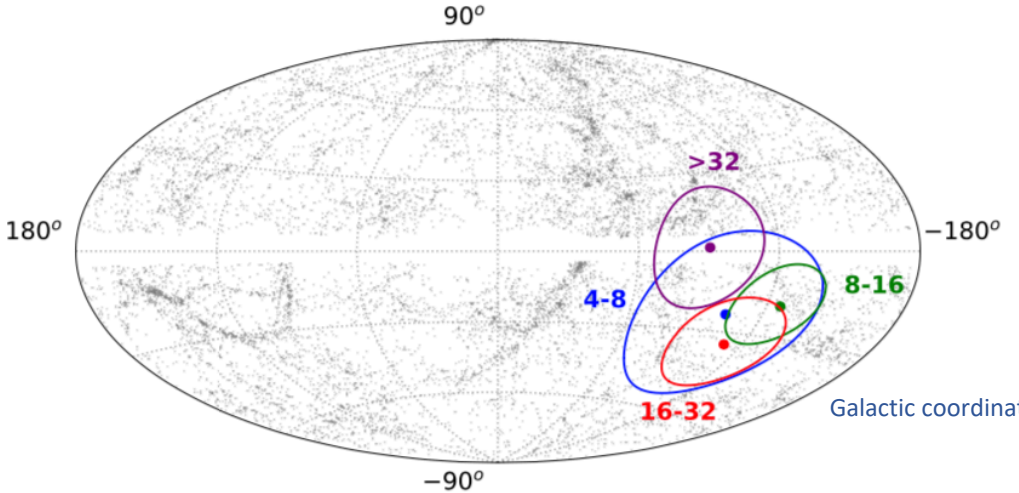

No clear trend in the evolution of dipole direction with energy

Dipole interpretation

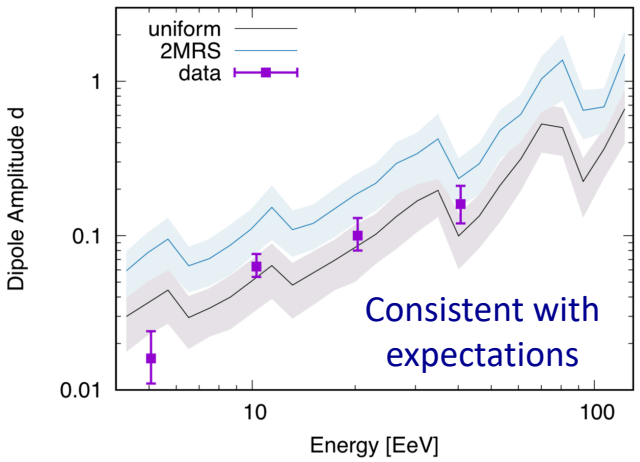

Models with mixed composition, $R_{max} = 6$ EV, source density 10^{-4} Mpc^{-3} from PRD 92 (2015) 063014

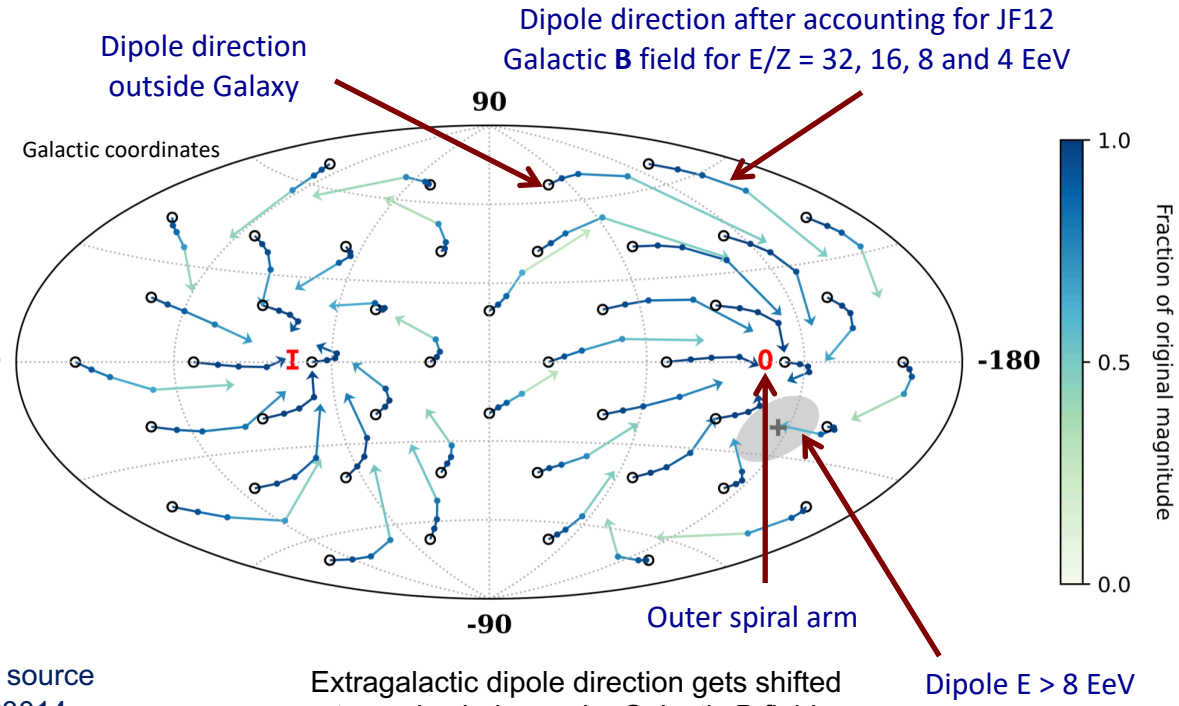

Extragalactic dipole direction gets shifted toward spiral arms by Galactic B field

Possibly due to the larger relative contribution from nearby sources to the flux at higher energies: extensive theoretical work (prediction and interpretation)

Giler et al. (JPhG 1980), Berezinsky et al. (A&A 1990), Harari et al. (PRD 2014), Harari et al. (PRD 2015), Globus & Piran (ApJL 2017), Wittkowski & Kampert (ApJL 2018), di Matteo et al. (MNRAS 2018), Hackstein et al. (MNRAS 2016), Hackstein et al. (MNRAS 2018), Ding et al. (ApJL 2021)

Search for Intermediate scale anisotropies

Analysis strategy

- Sky model probability maps:
- Null hypothesis H_0: isotropy $n^{H_0}(\mathbf{u}) = \dfrac{\omega(\mathbf{u})}{\sum_i \omega(\mathbf{u}_i)}$
- Single population signal model H_1:

$$s_j(\mathbf{u};\Theta) = \omega(\mathbf{u}) \times \phi_j a(d_j) \times \exp\left(\frac{\mathbf{u}\cdot\mathbf{u}_j}{2(1-\cos\Theta)}\right)$$

Φ_i = flux model x attenuat. model x ang. smearing (Θ) x exposure

$$n^{H_1}(\mathbf{u}) = (1-\alpha) \times n^{H_0}(\mathbf{u}) + \alpha \times \frac{\sum_j s_j(\mathbf{u};\Theta)}{\sum_i \sum_j s_j(\mathbf{u_i};\Theta)}$$

(free parameters: α and Θ)

- Test statistics: TS = 2 log(H_1/H_0) → $\mathrm{TS} = 2\sum_i k_i \times \ln \dfrac{n^{H_1}(\mathbf{u}_i)}{n^{H_0}(\mathbf{u}_i)}$
- p-value from Wilk's theorem: p(TS) = $p_{\chi 2}$(TS, ndf)

From catalogs to UHECR sky models

We study four cosmic rays sky models obtained from:

- **Near-infrared emission of galaxies (2MASS)**
  - Assuming UHECR luminosity proportional to stellar mass
- **Radio emission from starburst galaxies**
  - Assuming UHECR luminosity proportional to starforming activity
- **X-rays from AGNs (Swift-BAT)**
  - Assuming UHECR luminosity is driven by accretion onto super-massive black holes
- **γ-rays from jetted AGNs (Fermi-LAT)**
  - Assuming UHECR luminosity is proportional to the inner jet activity

Results

more than 2,600 ultra-high energy cosmic rays above 32EeV

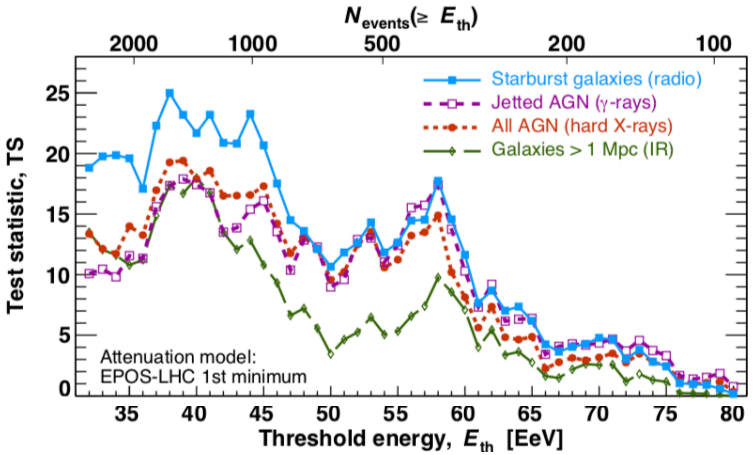

Catalog	$E_{\rm th}$ [EeV]	Fisher search radius, Θ [deg]	Signal fraction, α [%]	$\mathrm{TS}_{\rm max}$	Post-trial p-value
All galaxies (IR)	40	16^{+11}_{-6}	16^{+10}_{-7}	18.0	7.9×10^{-4}
Starbursts (radio)	38	15^{+8}_{-4}	9^{+6}_{-4}	25.0	3.2×10^{-5}
All AGNs (X-rays)	39	16^{+8}_{-5}	7^{+5}_{-3}	19.4	4.2×10^{-4}
Jetted AGNs (γ-rays)	39	14^{+6}_{-4}	6^{+4}_{-3}	17.9	8.3×10^{-4}
All galaxies (IR)	58	14^{+9}_{-5}	18^{+13}_{-10}	9.8	2.9×10^{-2}
Starbursts (radio)	58	18^{+11}_{-6}	19^{+20}_{-9}	17.7	9.0×10^{-4}
All AGNs (X-rays)	58	16^{+8}_{-6}	11^{+7}_{-6}	14.9	3.2×10^{-3}
Jetted AGNs (γ-rays)	58	17^{+8}_{-5}	12^{+8}_{-6}	17.4	1.0×10^{-3}

Results

Flux Map above 40 EeV

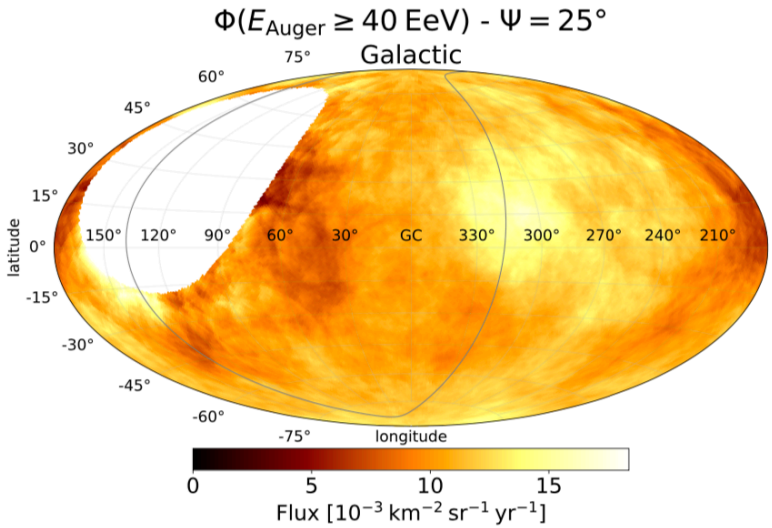

Best fit sky models above 40 EeV

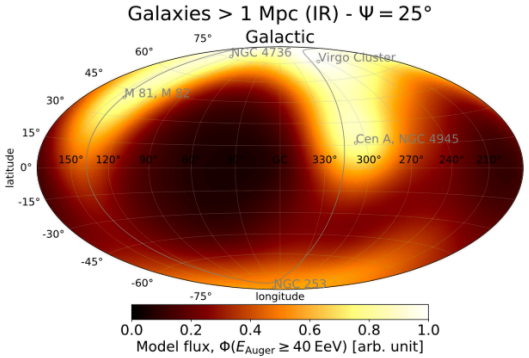

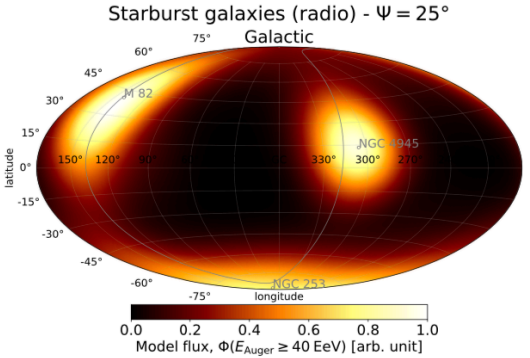

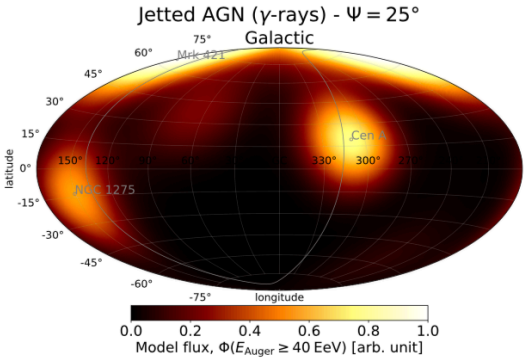

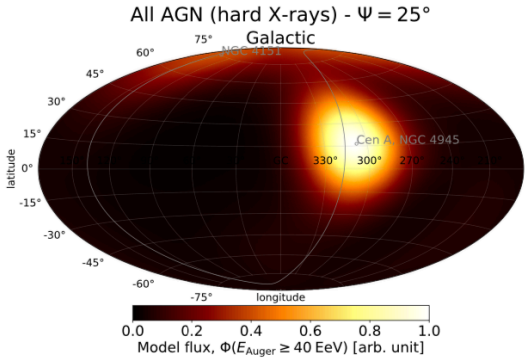

Note: sky maps do not include any isotropic component

The Centaurus Region

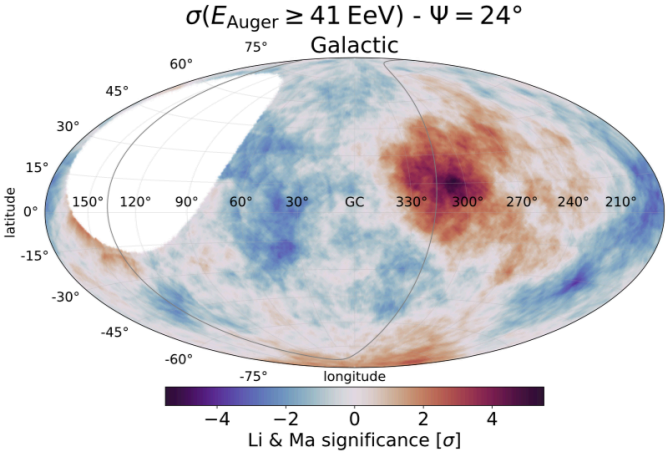

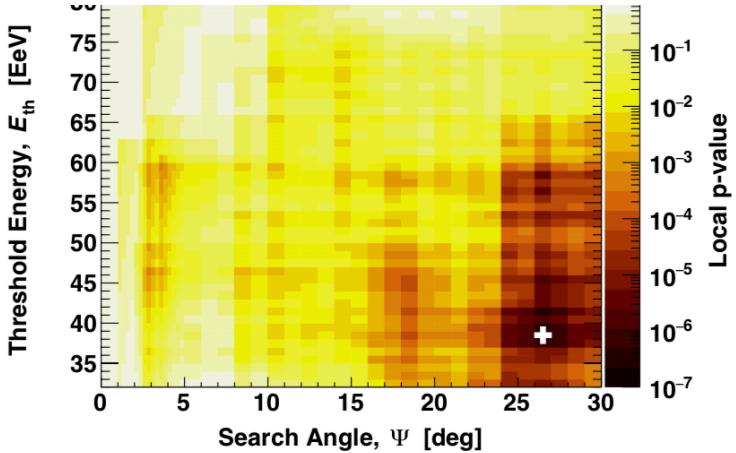

$log_{10}(R_{cut}/V) \approx 18.7$ from Auger best fit (2017)

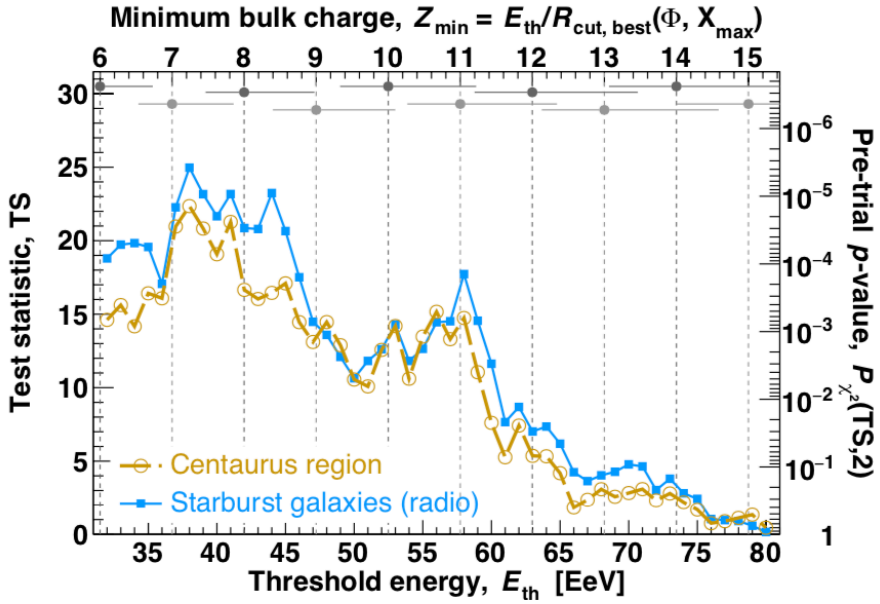

Conclusions

Large-scale anisotropies:

- The statistical significance of the large-scale dipolar modulation observed above 8 EeV has increased to 6.6σ, (p-value = 5.1×10^{-11}).

- The dipolar amplitude increases with energies although there is no clear trend in the change of the dipole direction as a function of energy.
  - Possibly due to the larger relative contribution from nearby sources to the flux at higher energies; Interpretation of the rec. dipole directions requires taking into account the magnetic deflections of the particles during their trajectories.

Intermediate-scale anisotropies:

- Evidence for a deviation in excess of isotropy at intermediate angular scale with ~ 15^{o} Gaussian spread or 25^{o} top-hat radius obtained at the 4σ significance level for cosmic-ray energies above ~ 40 EeV

Backup

Dipolar + quadrupolar reconstruction

Energy [EeV]	d_i	Q_{ij}
4-8	$d_x = -0.008 \pm 0.007$	$Q_{zz} = 0.008 \pm 0.036$
	$d_y = 0.008 \pm 0.007$	$Q_{xx} - Q_{yy} = 0.004 \pm 0.026$
	$d_z = -0.008 \pm 0.021$	$Q_{xy} = -0.01 \pm 0.01$
		$Q_{xz} = -0.02 \pm 0.02$
		$Q_{yz} = -0.008 \pm 0.017$
8-16	$d_x = -0.005 \pm 0.013$	$Q_{zz} = 0.074 \pm 0.064$
	$d_y = 0.045 \pm 0.013$	$Q_{xx} - Q_{yy} = 0.02 \pm 0.05$
	$d_z = 0.01 \pm 0.04$	$Q_{xy} = 0.039 \pm 0.024$
		$Q_{xz} = -0.002 \pm 0.031$
		$Q_{yz} = -0.03 \pm 0.03$

Quadrupolar amplitudes not significant and dipole components consistent with those obtained by assuming a pure dipole

Energy [EeV]	d_i	Q_{ij}
16-32	$d_x = 0.05 \pm 0.02$	$Q_{zz} = -0.14 \pm 0.14$
	$d_y = 0.09 \pm 0.02$	$Q_{xx} - Q_{yy} = 0.17 \pm 0.09$
	$d_z = -0.15 \pm 0.07$	$Q_{xy} = -0.05 \pm 0.04$
		$Q_{xz} = 0.12 \pm 0.06$
		$Q_{yz} = 0.06 \pm 0.06$
≥ 32	$d_x = -0.12 \pm 0.05$	$Q_{zz} = -0.17 \pm 0.26$
	$d_y = 0.11 \pm 0.05$	$Q_{xx} - Q_{yy} = 0.43 \pm 0.17$
	$d_z = -0.22 \pm 0.13$	$Q_{xy} = 0.10 \pm 0.09$
		$Q_{xz} = -0.12 \pm 0.11$
		$Q_{yz} = 0.13 \pm 0.11$
≥ 8	$d_x = -0.001 \pm 0.011$	$Q_{zz} = 0.02 \pm 0.06$
	$d_y = 0.06 \pm 0.01$	$Q_{xx} - Q_{yy} = 0.08 \pm 0.04$
	$d_z = -0.03 \pm 0.03$	$Q_{xy} = 0.02 \pm 0.02$
		$Q_{xz} = 0.02 \pm 0.03$
		$Q_{yz} = -0.003 \pm 0.026$

Quadrupolar amplitudes not significant and dipole components consistent with those obtained by assuming a pure dipole

Dipole reconstruction

E (EeV)	N	$d_\perp$	d_z	d	α_d [°]	δ_d [°]	$P(\geq r_1^\alpha)$
4-8	106, 290	$0.01^{+0.006}_{-0.004}$	-0.012 ± 0.008	$0.016^{+0.008}_{-0.005}$	97 ± 29	-48^{+23}_{-22}	1.4×10^{-1}
8-16	32, 794	$0.055^{+0.011}_{-0.009}$	-0.03 ± 0.01	$0.063^{+0.013}_{-0.009}$	95 ± 10	-28^{+12}_{-13}	3.1×10^{-7}
16-32	9, 156	$0.072^{+0.021}_{-0.016}$	-0.07 ± 0.03	$0.10^{+0.03}_{-0.02}$	81 ± 15	-43^{+14}_{-14}	7.5×10^{-4}
≥8	44, 398	$0.059^{+0.009}_{-0.008}$	-0.042 ± 0.013	$0.073^{+0.011}_{-0.009}$	95 ± 8	-36^{+9}_{-9}	5.1×10^{-11}
≥32	2, 448	$0.11^{+0.04}_{-0.03}$	-0.12 ± 0.05	$0.16^{+0.05}_{-0.04}$	139 ± 19	-47^{+16}_{-15}	1.0×10^{-2}

was 1.4×10^{-9} (ApJ 2020) and 2.6×10^{-8} (Science 2017)

Corresponds to 6.6σ

$E \geq 8$ EeV

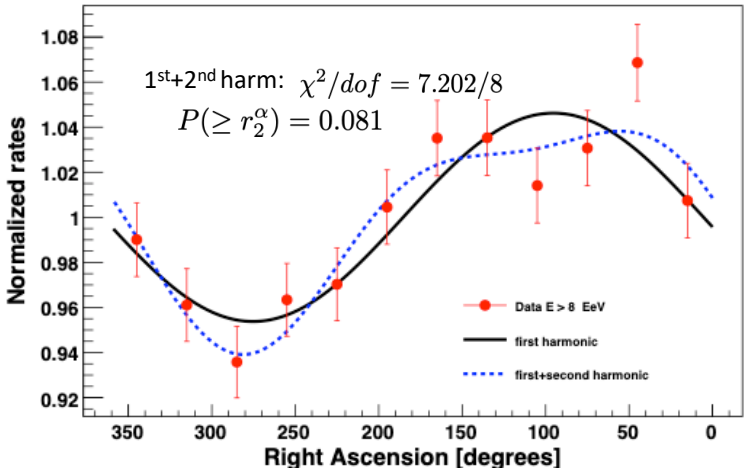

Smoothed by a top-hat window with 45° of radius

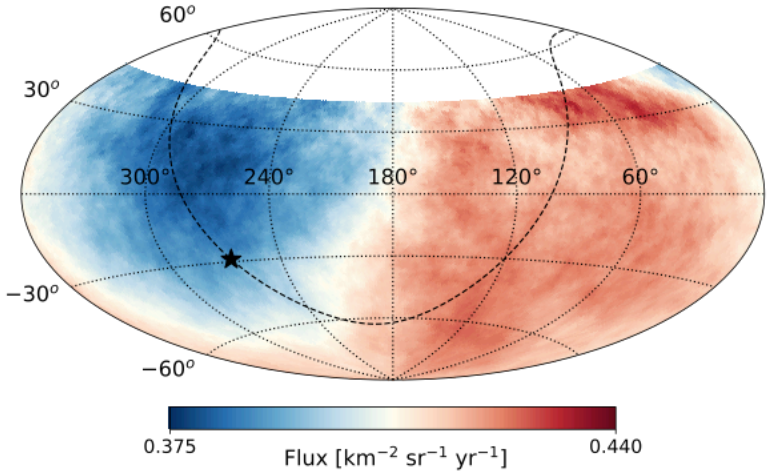

Dipole reconstruction E > 8 EeV

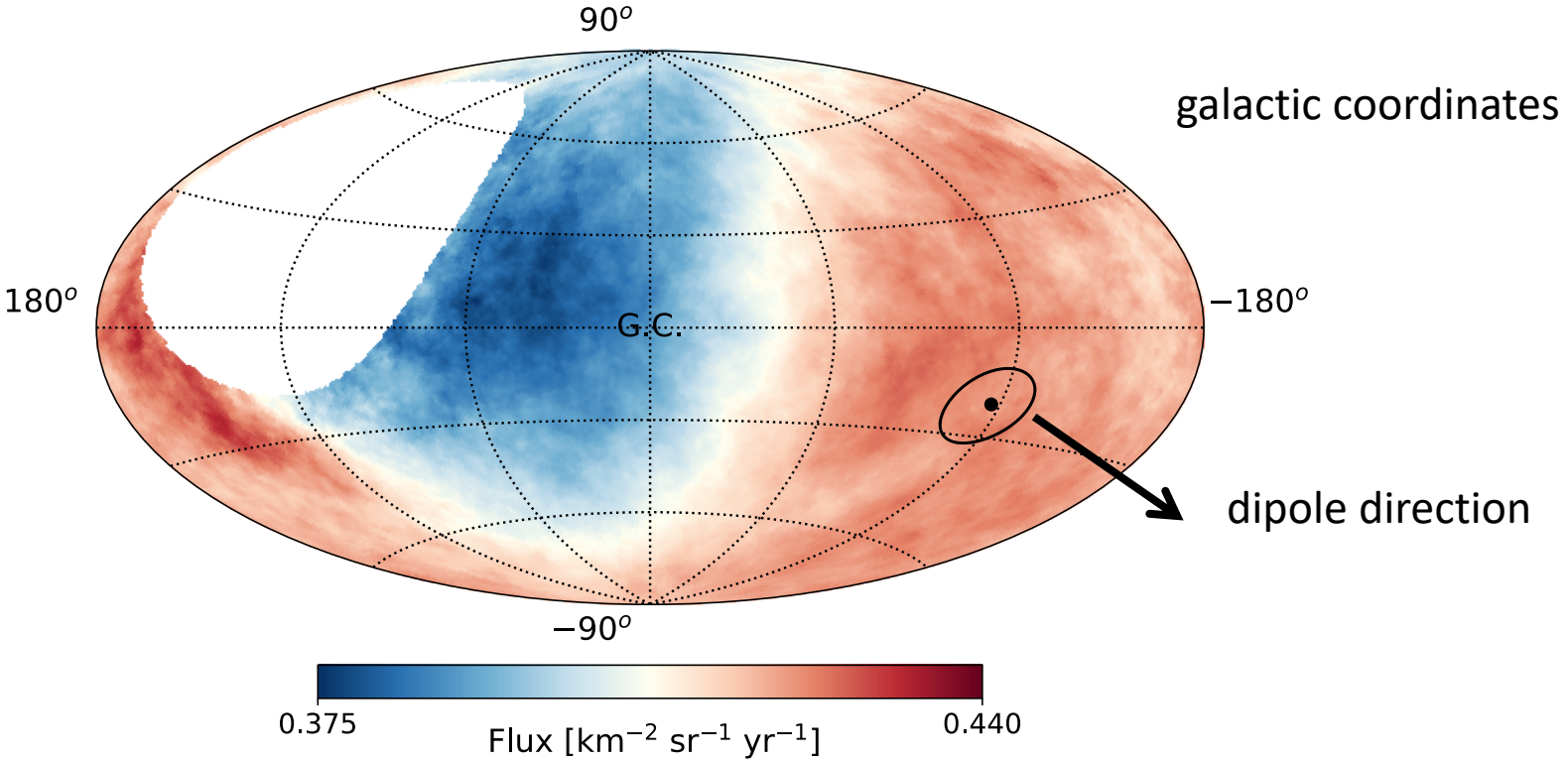

Dipole points to $(\mathrm{l}, \mathrm{b}) = \left(-117^{\circ}, -21^{\circ}\right)$ $\sim 115^{\circ}$ away from the direction of the Galactic center

Dipole reconstruction

Ratio between observed and expected events in windows of 45º

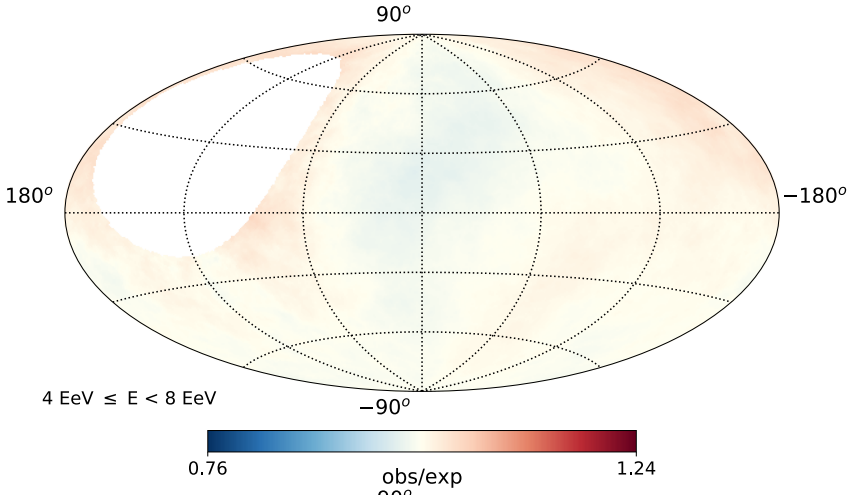

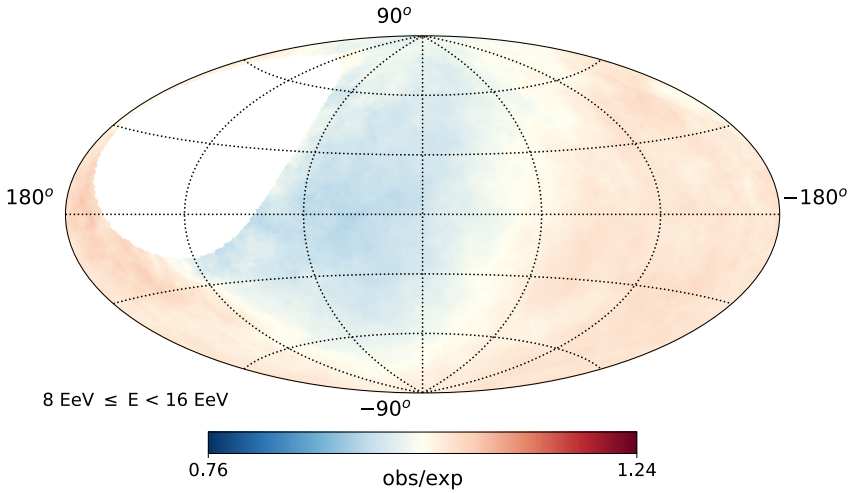

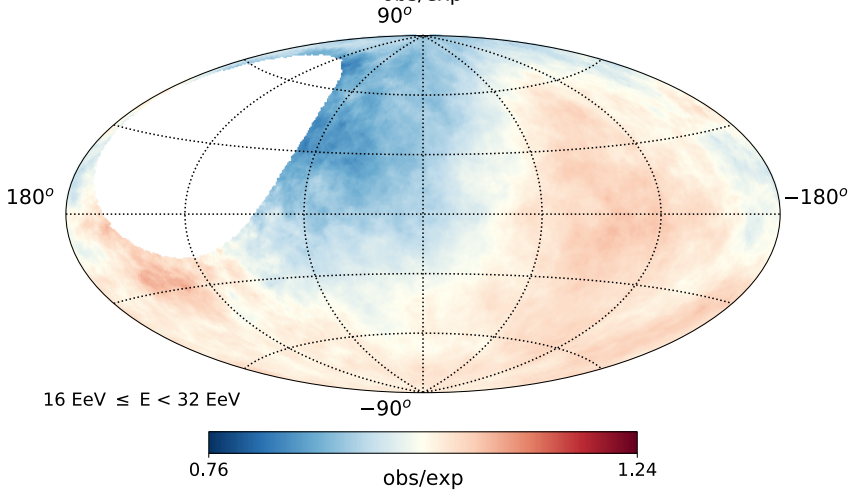

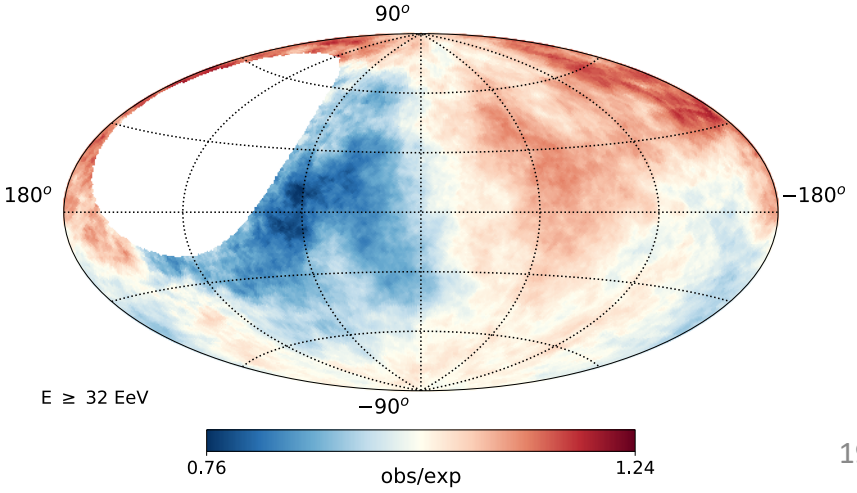

Results

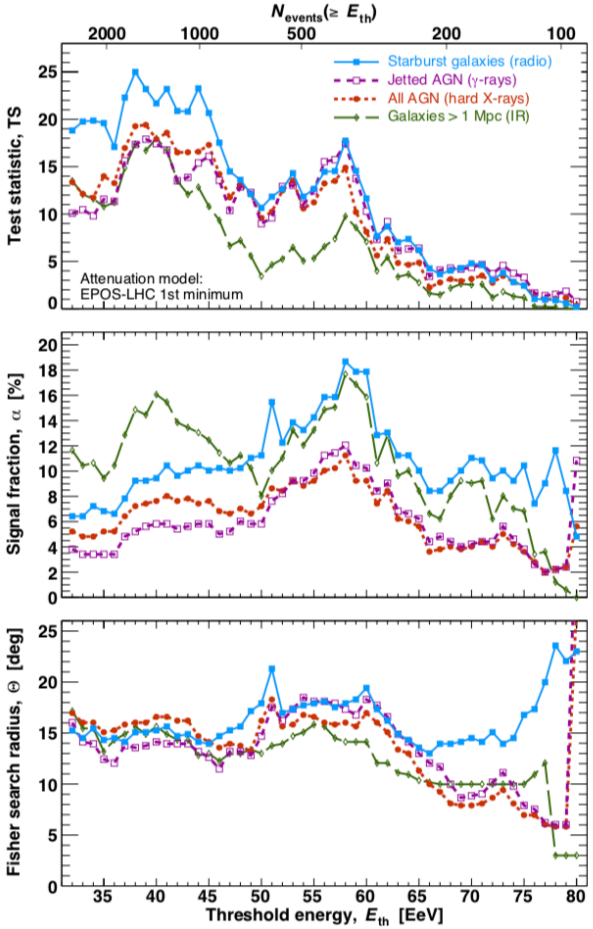
$N_{events}(\geq E_{th})$
2000
1000
500
200
100
Starburst galaxies (radio)
Jetted AGN (γ-rays)
All AGN (hard X-rays)
Galaxies > 1 Mpc (IR)
Test statistic, TS
Attenuation model:
EPOS-LHC 1st minimum
Signal fraction, α [%]
Fisher search radius, Θ [deg]
Threshold energy, E_{th} [EeV]

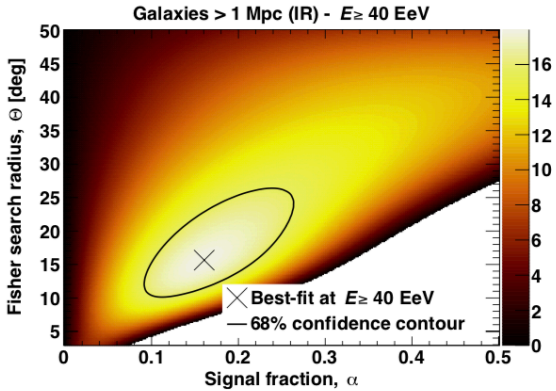
Galaxies > 1 Mpc (IR) - $E \geq$ 40 EeV
Fisher search radius, Θ [deg]
Signal fraction, α
Best-fit at $E \geq$ 40 EeV
68% confidence contour
TS = 2 ln L(α,Θ) / L(0,•)

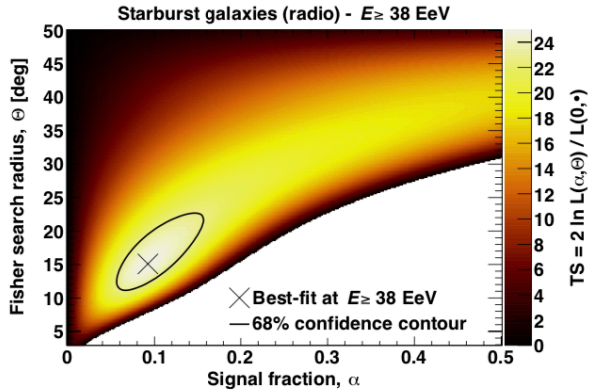
Starburst galaxies (radio) - $E \geq$ 38 EeV
Fisher search radius, Θ [deg]
Signal fraction, α
Best-fit at $E \geq$ 38 EeV
68% confidence contour
TS = 2 ln L(α,Θ) / L(0,•)

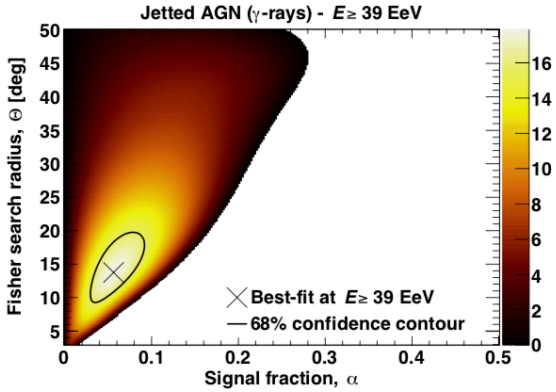
Jetted AGN (γ-rays) - $E \geq$ 39 EeV
Fisher search radius, Θ [deg]
Signal fraction, α
Best-fit at $E \geq$ 39 EeV
68% confidence contour
TS = 2 ln L(α,Θ) / L(0,•)

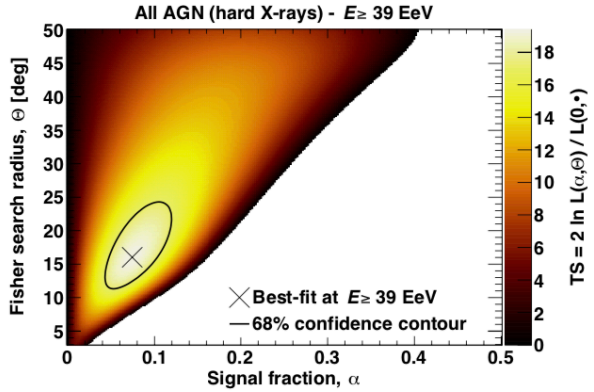
All AGN (hard X-rays) - $E \geq$ 39 EeV
Fisher search radius, Θ [deg]
Signal fraction, α
Best-fit at $E \geq$ 39 EeV
68% confidence contour
TS = 2 ln L(α,Θ) / L(0,•)

Evolution of test statistic

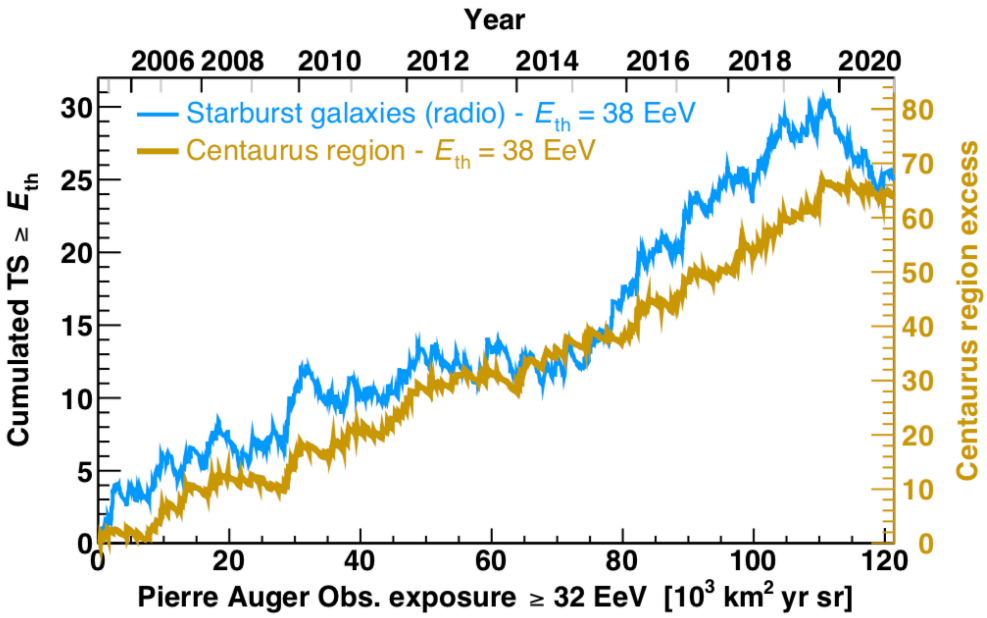

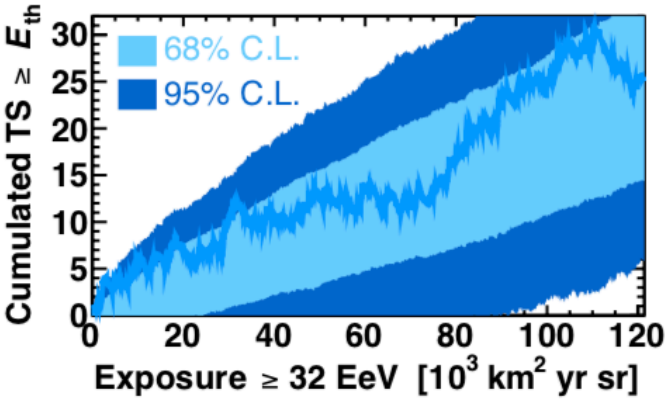

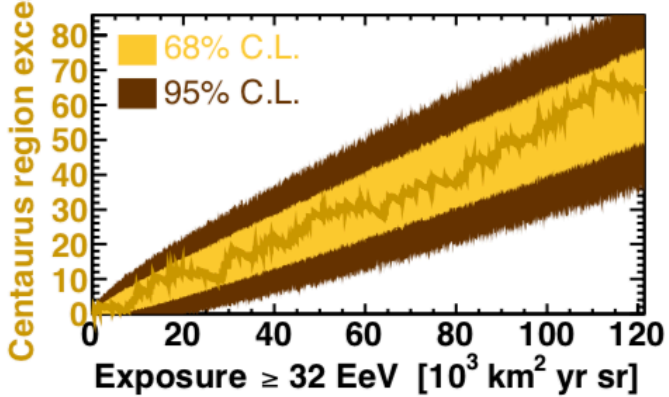

Assuming a fixed top-hat angular scale Ψ = 27° and a continued growth of the excess, the 5σ discovery threshold would be within reach by the end of 2025 (± 2 calendar years)